

# Introduction to Latest RF ATE with Low Test Cost Solutions

Masayuki KIMISHIMA<sup>†a)</sup>, Member

**SUMMARY** This paper describes latest RF Automated Test Equipment (RF ATE) technologies that include device under test (DUT) connections, a calibration method, and an RF test module mainly focusing on low cost of test (COT). Most important respect for low COT is how achieve a number of simultaneous measurements and short test time as well as a plain calibration. We realized these respects by a newly proposed calibration method and a drastically downsized RF test module with multiple resources and high throughput. The calibration method is very convenient for RF ATE. Major contribution for downsizing of the RF test module is RF circuit technology in form of RF functional system in package (RF-SIPs), resulting in very attractive test solutions.

**key words:** ATE, SoC tester, SIP, calibration, LTCC, MMIC

## 1. Introduction

By advanced CMOS-RF LSI, it is becoming possible to be one-chip integration of various wireless application such as wireless LAN and Bluetooth as well as cellular for 2G (GSM/EDGE), 3G (UMTS/WCDMA), and 3.9G (LTE) [1]–[3]. Also, multiple-input multiple-output (MIMO) topologies will become one of most promising solutions for improving the spectral efficiency of wireless systems [4], [5]. For ATE such as SoC testers, COT is vital as well as a measurement accuracy. Since the demand of reducing COT of RF test has been also increasing, simultaneous testing capability and higher throughput are becoming most important specifications for an RF ATE.

For these requirements, several technical aspects for an RF ATE should be concerned. With respect to DUT boards, the stable correlation and repeatability while simultaneous multi DUTs testing are often more important than to get extreme accurate data for low COT. A plane calibration method also contributes to low COT. Since there are many RF ports that should be calibrated periodically, calibration time and its complexity affect the rate of uptime of an RF ATE. We propose a new calibration method specialized for the RF ATE structure that derives a short calibration time with a plane operation. To implement RF multiple measurement resources with compact size, we constructed an RF front-end with RF functional system in package (RF-SIPs) instead of RF-HBICs. In addition, high speed switch MMICs for switches as well as for step attenuators using our accumulated GaAs high electron mobility trans-

sistor (HEMT) technology have been incorporated. These technologies bring multiple resources integration and high test throughput with compact module size. In following sections, we describe various kinds of technologies of latest RF ATE focusing on low test cost.

## 2. System Structure of RF ATE and Essential Issue with DUT Board Installation

### 2.1 Basic Structure of RF Test System

The photograph of our SoC test system and the basic construction of the test head for RF ATE are shown in Fig. 1 and Fig. 2, respectively. The SoC test system consists of the main frame, PC, and the test head. The main frame is a common instrument for various kinds of ATEs, and includes a fundamental DC power supplies and liquid cooling sources. PC is for operations of the whole ATE system based on the OS specialized for the ATE. The test head plays a most important role of ATE systems, it determines the per-

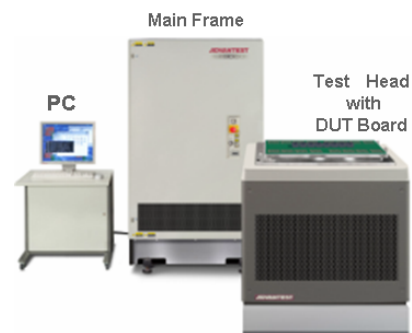


Fig. 1 SoC test system.

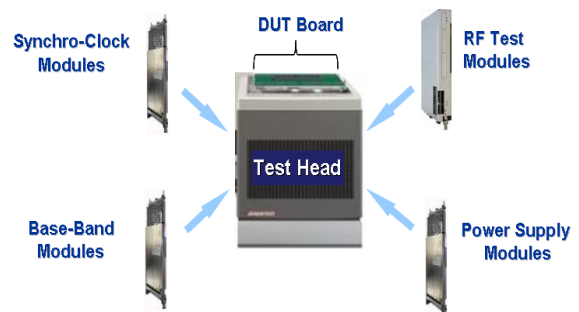


Fig. 2 Test head construction.

Manuscript received November 28, 2011.

Manuscript revised April 1, 2012.

<sup>†</sup>The author is with Gunma Research and Development Center, Advantest Corporation, Gunma-ken, 370-0718 Japan.

a) E-mail: masayuki.kimishima@jp.advantest.com

DOI: 10.1587/transele.E95.C.1147

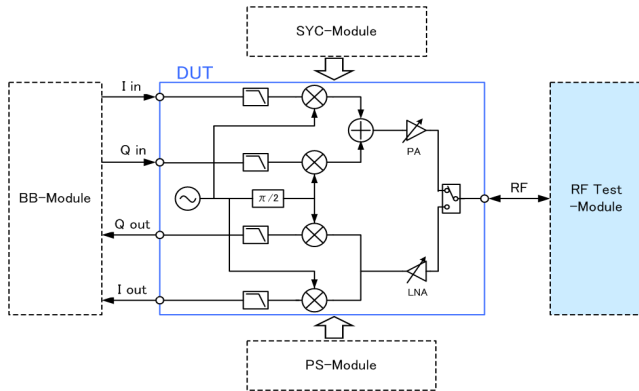


Fig. 3 Test diagram for transceiver devices.

performances of RF ATE for RF-ICs testing. The test head consists of various kinds of modules and the DUT board. A testing block diagram of the test head with the RF ATE is depicted in Fig. 3. For testing of RF-LSI, an RF test module, a base-band (BB) module, a power supply (PS) module, and a synchro clock (SYC) module are installed. In case of DUTs with digital functions, a high speed digital module is also installed according to the required speed. Test cost mainly depends on test time. Therefore, simultaneous multi-die measurements and higher throughput per die are very important. Especially, the RF test module is the key module and required to have simultaneous testing capability and higher throughput. A high density construction of our new RF test module is described in Sect. 3.

The DUT board is an interface between each modules and DUTs. Extremely, performances of the RF interface between the RF test module and DUTs is very important and a serious portion for the evaluation of DUT. Importance and difficulties on role of DUT boards associated with a calibration method is substantial respect of RF testing. Therefore, the design of DUT boards and developments of an RF calibration topology are also very important as well as the RF test module for reducing COT. Testing of RF-IC/RF-LSI includes an evaluation of digital and baseband functions as well as RF characteristics.

## 2.2 Main Issue for DUT Board

### Simultaneous multi die testing

In order to comply with the requirement of reducing COT, we have to confront difficulties of the simultaneous multi-die measurements of RF-ICs. With respect to DUT boards, most serious problem is a correlation error among multi-die measurements as shown in Fig. 4. Major causes for the correlation error among multiple sockets are designated by following:

- #1 Instability of socket pins to a DUT board contact
- #2 Instability of RF connectors to a DUT board contact
- #3 Imbalance of the pattern layout around the sockets
- #4 Variations of component values for RF parts

A time-varying correlation error occurs often due to socket

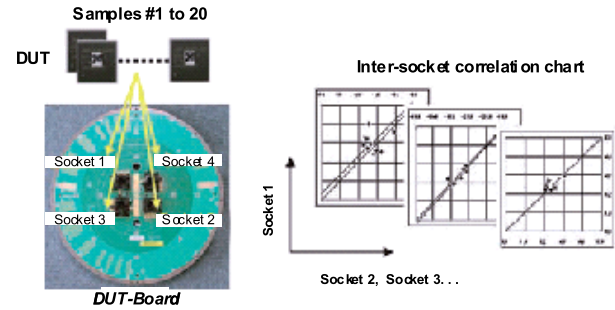


Fig. 4 Correlation among multiple sockets.

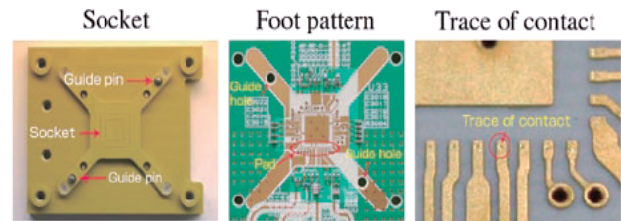


Fig. 5 Pin contact condition.

pins to DUT board contact. Imbalance of the RF patterns around the sockets and of the RF ground condition for transmission lines, and variations of component values in RF parts of the matching circuits for the DUTs might affect a DUT dependent correlation error.

To keep a stable correlation among simultaneous multi DUTs, each layout of RF transmission lines for DUTs which include RF ground condition and matching accuracy should be designed as similar as possible. Since stability of pin contacts with sockets is very important for the repeatability of measurement, the adequate shape and metal materials of the socket pins should be concerned. The pin contact check at regular interval during test is also indispensable. The pin contacts condition is shown in Fig. 5.

### Calibration

In a usual RF ATE, a calibration for correction of measurement errors is performed at module input/output (I/O) ports as reference planes. Then, an error correction between module I/O ports and DUTs is accomplished by embedding S-parameters of the DUT board with a corrective algorithm. The S-parameters must be known exactly, and then, implemented S-parameters should be valid during device testing. Above conventional calibration method has serious problems with the accuracy of error corrections and with the usability toward the operators. To guarantee the measurement accuracy of DUTs, a calibration should be executed at DUT ports as reference planes. Concerning these technical backgrounds, we proposed a new calibration technique that is executed by a combination of the standard calibration (STD-Cal) and the frequency domain reflectometry calibration (FDR-Cal). STD-Cal refers to the calibration at module I/O ports using open-short-load (OSL) method. As demonstrated in Fig. 6 and Fig. 7, FDR-Cal is the correction of transmission characteristics between module I/O ports and

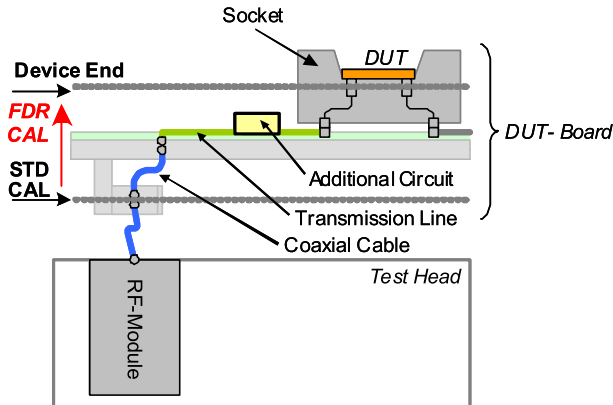


Fig. 6 Definition of calibration reference plane.

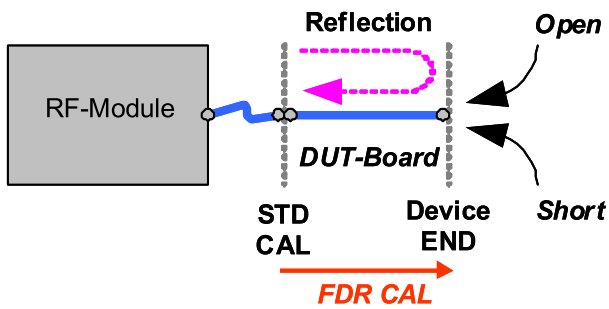
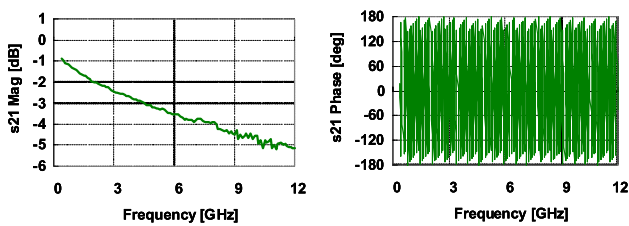
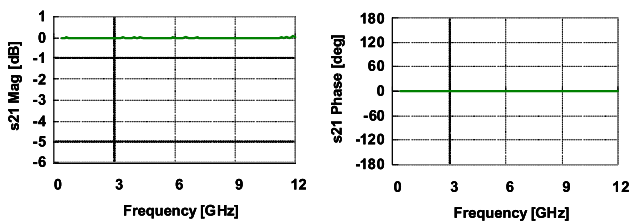


Fig. 7 Reflection method.



(a) Before FDR Cal.



(b) After FDR Cal

Fig. 8 Verification of calibration algorithm.

DUT ports, using open-short (OS) method at DUT ports of the sockets. FDR-Cal allows moving calibration planes from module I/O ports to DUT ports with an easy process.

The verification of the new method is demonstrated in Fig. 8. By comparison before FDR-Cal and after FDR-Cal, it can be confirmed that this calibration method is very plain

and effective for RF ATE. Consequently, low COT can be achieved by higher rate of uptime of RF ATE.

### 3. RF Test Module

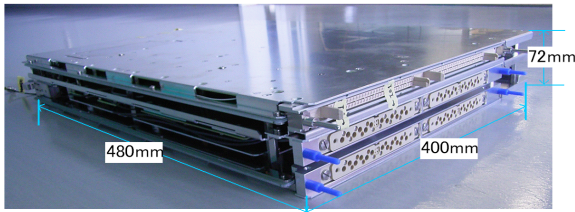
#### 3.1 Conventional RF Test Module

In recent trend of an RF testing, the demands for more multiple channel resources and higher throughput per channel are rapidly increasing. Our conventional RF test modules are composed of many RF-HBICs. An RF-HBIC is a large size high frequency component with coaxial connectors. And each of RF-HBICs is connected with RF cables such as semi-rigid cables. Therefore, the dimension of a module becomes large, and it becomes extremely difficult to install multiple resources into one module with small size. In addition, RF attenuators that use mechanical RF switches have disadvantages of slow settling time besides large size. The slow settling time cause low throughput. Our conventional RF test module consists of one vector signal generator (VSG) for a modulated signal generation, one vector signal analyzer (VSA) for a modulated signal analysis, and four vector network analyzers (VNA). In spite of non full multiple resources, dimension of the RF test module becomes large size as 400 mm × 480 mm × 262 mm.

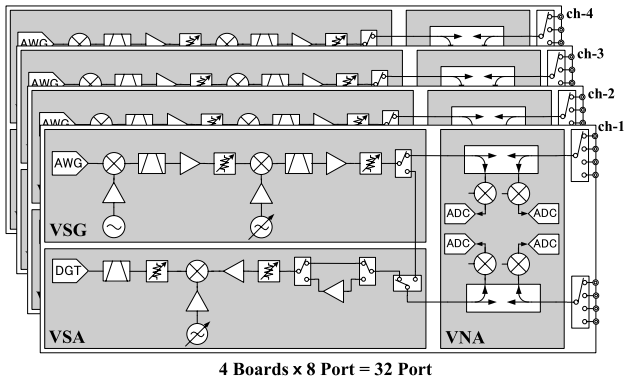
For these reasons, we have been facing difficulties in the realization of small size RF test module with complete 4 channel simultaneous measurement and high throughput per channel.

#### 3.2 Advantage of New RF Test Module

To overcome the problems mentioned above, we composed RF front-end of the new RF module with the RF-SIPs using LTCC substrates instead of RF HBICs, and then, the RF test module is drastically downsized [6]. LTCC circuits are very adequate solution for small and medium volume applications [7], [8]. With regard to high throughput performances, we succeeded in the integration of RF step attenuator and single pole, four throw (SP4T) switch on one SIP by use of the developed high-speed step attenuator MMICs and SP4T switch MMIC, respectively. The high-speed MMICs can improve throughput of the RF test module, as being described in Sect. 4. An appearance of the new RF test module is shown in Fig. 9(a). It is equipped with 4 channels for each of the resources of VSG, VSA and VNA. 2-tone signal output function is provided in the VSG. The resource construction is shown in Fig. 9(b). The innovative RF-SIPs realize an RF test module that provide a 4 channel simultaneous full RF function measurement with volume of 480 mm × 400 mm × 72 mm. Since 4 resources are entirely independent, they can be assigned to the individual DUTs. Figures 10 and 11 show multi-task capabilities performed by the 4 resources. In case of the testing for identical DUTs, each different test procedure can be executed. In the testing with different type of DUTs, the different test program can



(a) Module



(b) Resource

Fig. 9 Structure of new RF test module.

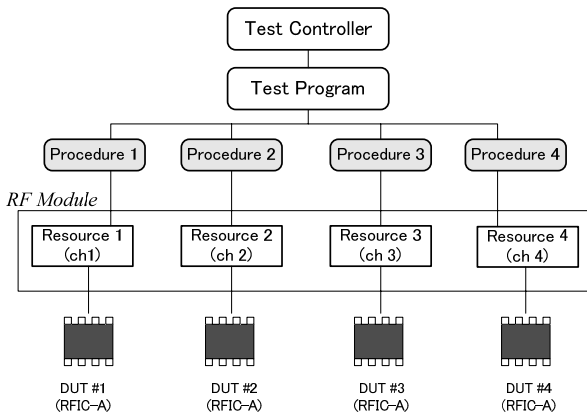


Fig. 10 Module slice test performance—Testing same type of DUTs with different procedure.

be applied for each DUT. These functions are called “module slice” having an adaptive test capability and a multi-task test that provide decreasing test time and an effective test debug. Furthermore, throughput per channel is significantly improved as compared with our conventional RF test module.

3.3 RF-SIP and RF Board Construction

The RF front-end featuring large size metal housing package RF-HBICs with RF-connectors and coaxial cables brings excellent performances of isolation and transmission characteristics. On the other hand, the new configuration in form

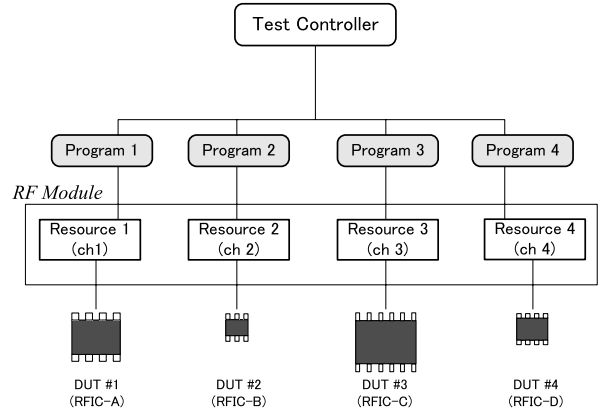


Fig. 11 Module slice test performance—Testing different DUTs with different program.

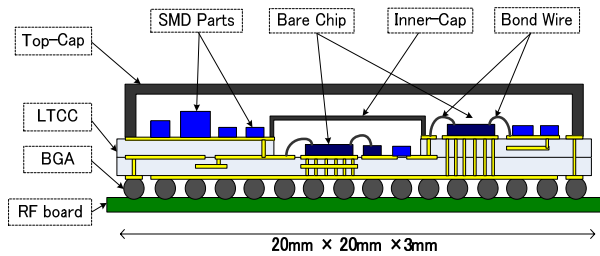


Fig. 12 Structure of RF-SIP.

of RF-SIPs and RF boards has several design considerations for RF performances. Especially, problems of isolation between inner circuits of RF-SIPs, and mismatch in ball grid array (BGA) connection between RF-SIPs and RF board are serious issues. The RF-SIP structure that realizes good isolation and passive circuit integrations is depicted in Fig. 12.

In this concept, semiconductor bare chip devices of high isolation required are mounted into small cavities of the LTCC substrate. The cavity is electrically sealed with inner metal cap whose rim is connected to ground through via holes. All of bare chips are mounted on the LTCC with face-up configuration, and are connected to microstrip lines using Au bond wires. Employing this SIP configuration, it is available to use various kinds of commercial and custom designed bare chips such as GaAs MMICs, Si-RFICs, and discrete devices. The SIPs also include several kinds of surface mount devices (SMD) to implement bias circuits and control circuits. 1005 and 0603 size SMD parts are mainly used. Precise RF passive circuits such as directional couplers, band-pass filters (BPFs) are also integrated inside of LTCC with strip line constructions. The SIPs are attached to the RF board using a solder reflow process with BGA inserted between the SIPs and RF board. RF ground vias are arranged around RF signals to achieve a good impedance match and an enough isolation of RF signals. And many ground via are placed in around the center area of the LTCC to obtain the good RF ground condition and the thermal radiation as much as possible. As all kinds of SiPs are designed according to the same PIN assignment, we can evalu-

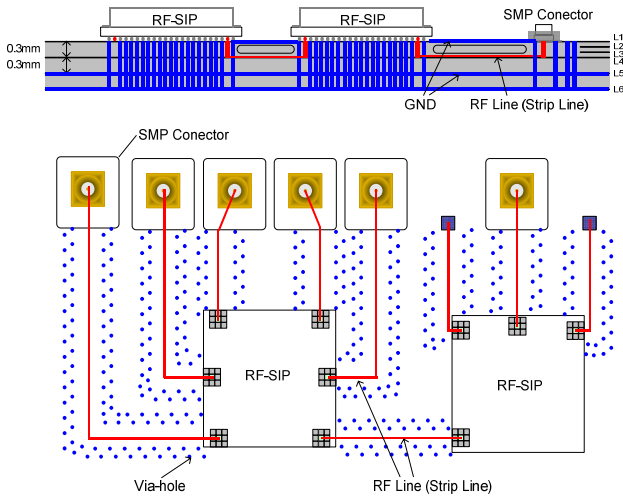


Fig. 13 Structure and pattern lazyout of RF board.

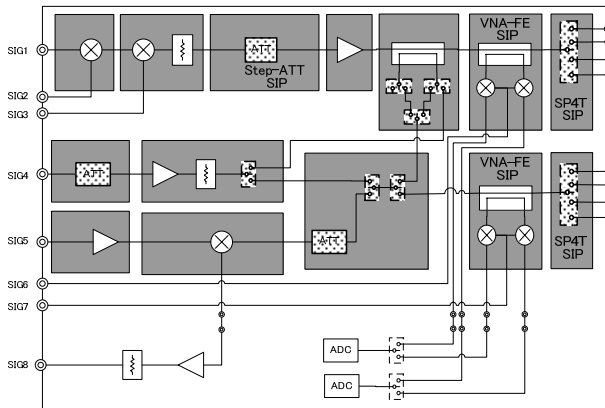


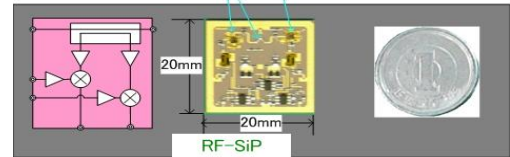
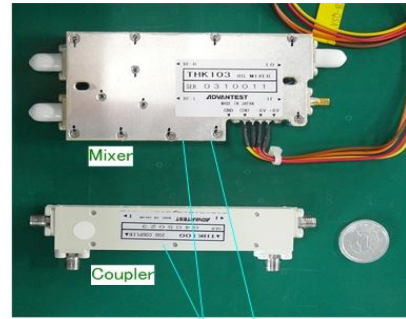
Fig. 14 Block diagram of RF board.

ate them with the particularly designed common RF socket.

Figure 13 demonstrates pattern layout of the RF board. The RF transmission lines are strip line structure. The strip line structures, in which the RF signal is transmitted through an inner layer pattern, can achieve higher isolation than microstrip lines. As with LTCC substrate, at area of the RF pattern, many ground via holes are deposited in short pitch in order to suppress waveguide mode and parallel plate mode. Dimension of all the RF-SiPs mounted on the RF boards is 20 mm × 20 mm × 3 mm. 14 RF-SiPs are mounted per one RF board as shown in Fig. 14.

### 3.4 Down Sizing Example of RF SiP

Figure 15 exhibits the comparison of the RF HBIC and the RF SiP. Each of them has the same function as VNA including one directional coupler, two isolation amplifiers, and two down convert mixers. By applying RF SiP, the volume of VNA function block can be drastically down sized less than 1/66 compared with our conventional RF HBIC.



RF HBIC (Above Figure)  
 Coupler : 20 mm x 90 mm x 13 mm  
 2 Mixers + 2 Amplifiers : 48 mm x 90 mm x 13 mm  
 RF SiP (Below Figure)  
 Coupler + 2 Mixers + 2 Amplifiers : 20 mm x 20 mm x 3 mm

Fig. 15 Comparison of RF HBIC and RF SiP.

## 4. High Speed Switch Technologies for High Throughput

To realize high throughput of the RF test module, high-speed switching operation of switches for transmission path control and step attenuators for RF power level control is one of most important characteristics. In addition, high isolation is also very important for switches and step attenuators. HBICs using discrete bare chips are very attractive to achieve high isolation performance, but are not suitable for compact size. PIN diode switches are usually used for measurement instruments because of their fast switching performance, but they do not accomplish the requirements of smaller size and lower power consumption. GaAs MMIC switches are suitable for compact size and small power consumption, but are not adequate for fast switching required for ATE. To eliminate these dilemmas, we realized high speed switch MMICs and step attenuator MMICs using newly established HEMT process having on/off settling times on the order of several microseconds.

### High-speed switching HEMTs

As shown in Fig. 16, the settling time definition for RF ATE is the time required for the output power to go from 0 to 99.9% when the control voltage is switched. For the switches using conventional HEMT devices, the settling time from 10 to 90% is very fast in order of a few nanoseconds. However, at 0 to 99.9%, a well-known phenomenon called gate lag caused delays in order of several milliseconds to as long as several seconds. In order to obtain high throughput of RF test, it is crucial that all the circuits have fast switching times. Then, we developed a proprietary HEMT process based on the particular deposition technol-

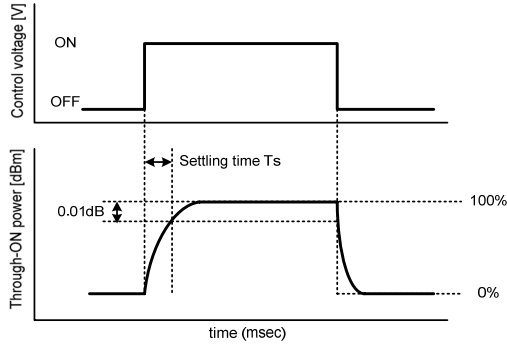


Fig. 16 Definition of settling time.

Table 1 Comparison of settling time for HEMTs.

		This Work	Conventional HEMT		
			Our HEMT	Product A	Product B
Settling Time	10-90%	3nsec	3nsec	1nsec	3nsec
	0-99.9% ( $\pm 0.01$ dB)	50usec	140msec	1.5msec	2sec

ogy for a passivation layer that derives significant improvement on switching speed. Table 1 presents a comparison of settling time for HEMT devices. The new type one has a settling time of about 50  $\mu$ s.

High speed switch and step attenuator MMICs

The designed two types of switch MMICs and three types of step attenuator MMICs are indicated by shading in the illustration of Fig. 14. Selects of transmission path are performed by two types of switches, single pole, double throw (SPDT) switches and single pole, four throw (SP4T) switches. For signal level control, on the other hand, three types of step attenuator with an attenuation of 40 dB, 35 dB, and 28 dB are used. The frequency range of MMICs is 100 MHz to 12 GHz.

Figures 17 and 18 show photographs of the SP4T switch and the 35 dB step attenuator MMICs. Both chip size are 1.2 mm  $\times$  2.4 mm. The configuration employs an elementary combination of series/shunt HEMT devices. Figure 19 exhibits the measured and simulated insertion loss and isolation of the SP4T switch. It can be seen that there is close between the measured and simulated results. The insertion loss of less than 1.8 dB and the isolation of more than 63 dB are achieved across a frequency band of 100 MHz to 12 GHz.

Figure 20 indicates the switching speed of the SP4T switch. The settling time is 50  $\mu$ sec, which is the same as for the HEMT devices themselves, and exhibit a significant improvement as compared with the conventional switches. The newly designed five types of MMICs have same high speed switching performance. The designed 40 dB, 35 dB, and 28 dB step attenuator have also very first switching speed same as switch MMICs.

Thanks to these high speed MMICs, and by adding improvement of frequency settling of the RF synthesizer,

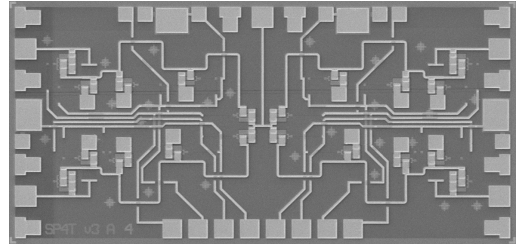


Fig. 17 Photograph of SP4T-switch.

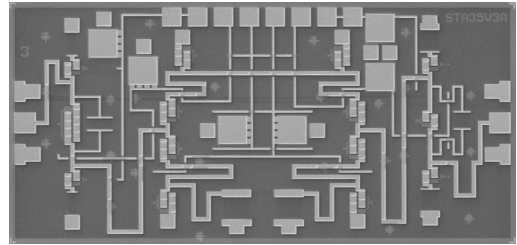


Fig. 18 Photograph of 35 dB step attenuator MMIC.

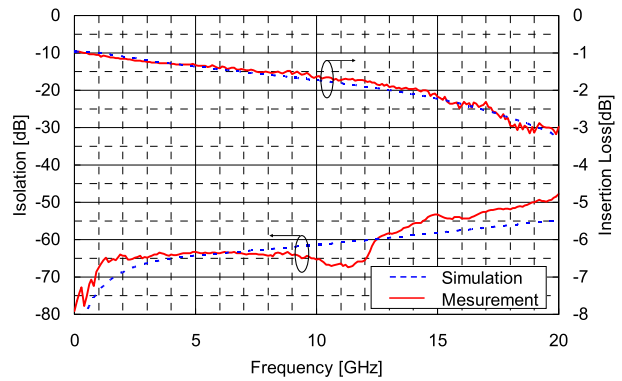


Fig. 19 Measured and simulated result of SP4T switch.

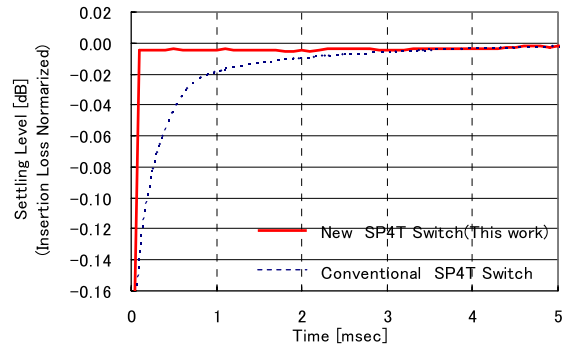


Fig. 20 Switching speed of SP4T switch.

the throughput per channel becomes less than 1/5 compared with our conventional module.

5. Performances of the RF ATE

Table 2 summarizes typical specifications of the RF ATE.

**Table 2** Typical specification of the RF ATE.

Common Term	Number of Channel per Module	4ch	
	RF Port per Module	I/O : 4port/ch, O : 4port/ch	
	Bidirectional Measure Only	16port 16port	
Signal Generation	Frequency Range	100M-6GHz	
	Level Range	-120~+8dBm(~2.5GHz) -120~+5dBm(~6GHz)	
	Level Accuracy	±0.9dB @6GHz 0~-60dBm	
	Modulation BW	40MHz	
	C/N	-99dBc/Hz @High Speed Mode, 6GHz(1MHzoff) -128dBc/Hz @High C/N Mode, 6GHz(1MHzoff)	
	Level + Frequency Settling	450us @High Speed Mode 20ms @High C/N Mode	
	EVM (WCDMA)	<=3.2%, -10dBm @High Speed Mode <=2%, -10dBm @High C/N Mode	
	EVM (802.11a)	<=2.2%, -10dBm @High C/N Mode	
Signal Measurement	Frequency Range	100M-12GHz	
	Maximum Power Level	+17dBm	
	Modulation BW	40MHz	
	C/N	-107dBc/Hz @High Speed Mode, 6GHz(1MHzoff) -134dBc/Hz @High C/N Mode, 6GHz(1MHzoff)	
	Frequency / Level Settling	300us @High Speed Mode 20ms @High C/N Mode	
	Level Accuracy	1.1dB, 12GHz, @-25dBm	
	Noise Floor	ATT Min(0dB), LNA off -141dBc/Hz, 2.5GHz ATT Max-add 32dB -111dBc/Hz, @2.5GHz LNA On, ATT 0dB -153dBm, @2.5GHz	
	EVM (WCDMA)	1%, -10dBm @High Speed Mode	
		EVM (802.10a)	1.5%, -10dBm @High Speed Mode
	Noise Figure Measurement	Frequency Range	600M-2.5GHz
ENR Range		0 to 20, 5dB Step	
ENR Accuracy		<1dB	
On/Off Settling		<150us	
ENR Settling		<500us	
Vector Analysis	Number of VNA port per Module	32	
	Frequency Range	400M-12GHz	
	Accuracy	<0.1dB	
	Directivity	10dB	

For the VSG, the minimum output power of less than -120 dBm and the maximum output power of more than +5 dBm are achieved across a frequency band of 100 MHz to 6 GHz. The noise floor of the VSA is -153 dBm at 2.2 GHz. As compared with our conventional RF test module, the settling time at the instantaneous frequency change is extremely improved from 800 μs to 150 μs.

**6. Conclusions**

In this paper, we introduced recent RF ATE technologies which include the DUT board, the calibration method as well as high density construction of RF test module. The RF test module is a fully 4 channel of VSA, VSG, and VNA having 32-ports with dimension of 480 mm × 400 mm × 72 mm. The volume is reduced about of 1/15, and the throughput per channel becomes less than 1/5 compared with our conventional module. Our new RF ATE will enable to reduce COT drastically, and provide convenient testing solutions featuring the adaptive test and the multi-task test by full resources structure.

**References**

[1] R. Koller, T. Ruhlicke, D. Pimingsdorfer, and B. Adler, "A single-chip 0.13 μSIPOS UMTS W-CDMA multi-band transceiver," 2006 IEEE Radio Frequency Integrated Circuits Symposium, June 2006.  
 [2] J.-W. Lai, C.-H. Wu, A. Lin, W.-K. Hong, C.-Y. Wang, C.-H. Shen,

Y.-H. Lin, Y.-H. Cho, Y.-C. Chen, and Y.-H. Chung, "A world-band triple-mode 802.11a/b/g SOC in 130-nSIPOS," IEEE J. Solid-State Circuits, vol.44, no.11, pp.2911-2921, Nov. 2009.  
 [3] A. Mirzaei, H. Darabi, A. Yazdi, Z. Zhou, E. Chang, and P. Suri, "A 65 nm CMOS quad-band SAW-less receiver SoC for GSM/GPRS/EDGE," IEEE J. Solid-State Circuits, vol.46, no.4, pp.950-964, April 2011.  
 [4] A. Yoshimoto and T. Hattori, "Area coverage of a multi-link MIMO system with water filling power allocation strategy," VTC-2007 Fall. 2007 IEEE 66th, pp.1137-1141, Sept. 30 2007-Oct. 3 2007.  
 [5] K. Lim, S. Min, S. Lee, J. Park, K. Kang, H. Shin, H. Shim, S. Oh, S. Kim, J. Lee, C. Yoo, and K. Chun, "A 2×2 MIMO tri-band dual-mode direct conversion CMOS transceiver for worldwide WiMAX/WLAN applications," IEEE J. Solid-State Circuits, vol.46, no.7, pp.1648-1658, July 2011.  
 [6] M. Kimishima, "Introduction to latest RF test technologies in RF ATE for low test cost," 2011 China-Japan Joint Microwave Conference Proceedings, April 2011.  
 [7] Y.C. Lee, W.I. Chang, and C.S. Park, "Monolithic LTCC SiP transmitter for 60 GHz wireless communication," 2005 IEEE MTT-Symp. Digest, pp.1015-1018, 2005.  
 [8] T. Baras and A.F. Jacob, "Integrated LTCC synthesizer and signal converter module at K-band," IEEE Trans. Microw. Theory Tech., vol.57, no.1, pp.71-79, Jan. 2009.



**Masayuki Kimishima** received the B.S. degrees in Electrical Engineering from Niigata University, Niigata, Japan. He joined Tokyo Keiki Inc. in 1984, where he was involved in the development of broadband microwave circuits for aero-defense systems. In 1994, he joined New Japan Radio Corporation, where he has worked on the development of MMICs for mobile communications. In 1998, he moved to ADVANTAST Corporation, where he has been engaged in the development of microwave and millimeter-wave MMIC for measurement instruments, and automated test equipments. He is a member of the IEEE.